

Valence-band structure of alkali halides determined from photoemission data

G. K. Wertheim, J. E. Rowe, D. N. E. Buchanan, and P. H. Citrin

AT&T Bell Laboratories, Murray Hill, New Jersey 07974

(Received 12 December 1994)

Valence-band photoemission spectra from a variety of alkali halides are shown to be well represented by a phonon-broadened density-of-states histogram with well-determined bandwidths and three or four main peaks. The bandwidths are generally in good agreement with band-structure calculations. The phonon broadening is typically 85% of that calculated for anion core levels, indicating that the valence-band holes are localized.

I. INTRODUCTION

It has been repeatedly noted¹⁻⁵ that x-ray and ultraviolet photoemission spectra from the valence bands of alkali halides are typically much broader than indicated by band-structure calculations. Even the presence of the spin-orbit splitting, which emerges clearly in ultraviolet absorption spectroscopy,⁶⁻⁸ has been questioned.² Only in the case of LiF,⁹ where the bandwidth is quite large, has qualitative agreement been demonstrated. Ultraviolet absorption and reflection spectroscopy measurements have traditionally provided the critical test of band-structure calculations, but to date they have failed to define the width of the valence band. We demonstrate here that a straight-forward analysis of photoemission valence-band data provides structures and widths that are characteristic of the true density of states (DOS).

Recent photoemission studies of shallow cation core levels in alkali halides^{10,11} have demonstrated that the core-level spectra are fully defined by the core-hole lifetime and phonon widths of bulk and surface components. This provided an incentive to explore whether the valence-band spectra could be interpreted using the same techniques. Our analysis shows that an appreciable fraction of the photoemission valence-band width is indeed due simply to phonon broadening,^{12,13} and that this broadening is comparable in magnitude to that calculated for halide core levels.^{11,14} In optical spectroscopy, phonon broadening is much weaker because the excitation does not produce a charged final state. As a result, optical-absorption data contain much more detail than those from photoemission. Although phonon broadening in insulators (and semiconductors) is a fundamental impediment for obtaining valence-band information from raw photoemission data, we find that a histogram containing the essential features of the DOS can be readily determined. Our approach is not only simple, but it ultimately allows meaningful comparison with band-structure calculations and yields reliable estimates of the bandwidths.

II. EXPERIMENTAL PROCEDURE

The experiments were carried out on thin, evaporated films of alkali halides supported on conducting or semi-

conducting substrates, as previously described.¹⁰ Most of the photoemission measurements were made with He I resonance radiation, but the Na salts were also examined with synchrotron radiation using the Bell Laboratories-Brookhaven 6-m toroidal grating monochromator beamline at the National Synchrotron Light Source. The total instrumental resolution was 0.10 eV in the work with He I radiation and slightly larger in the synchrotron work. Since the phonon widths are 5-10 times larger than the instrumental resolution, the spectra are not significantly broadened by instrumental effects. The data obtained, see Fig. 1, are similar to those previously published,¹⁻³ but have better resolution and less noise. Well-resolved structure was observed only in the iodides. The binding energies are referenced to the vacuum level,

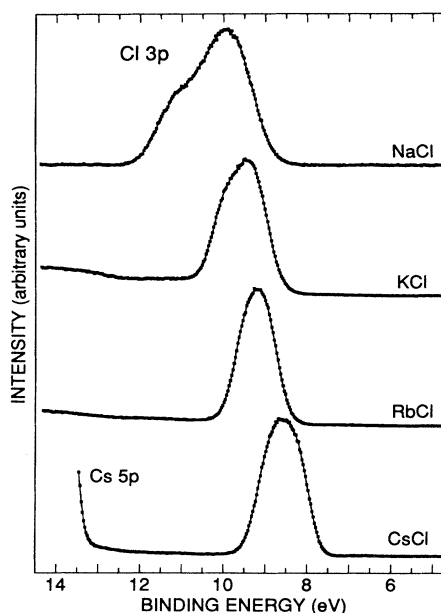


FIG. 1. Valence-band spectra of the chlorides of Na, K, Rb, and Cs. The NaCl data were taken with 75-eV synchrotron radiation and a sample temperature of 500 K. All other data were obtained with He I resonance radiation from room-temperature samples. Solid line is drawn through data as a guide to the eye.

which was determined by adding the photon energy to that of the cutoff at low kinetic energy.

The detailed structure of the valence-band DOS is greatly diminished in these data because the phonon broadening lies between 0.5 and 1.0 eV. In order to obtain information about the DOS, methods very different from those used in the analysis of core-level spectra are required. For core levels of insulators, the fundamental line shape is a phonon-broadened Lorentzian. For the valence band, the lifetimes width is negligibly small because there are no occupied states above the valence band. This simplifies the analysis somewhat, but the anion p states are spread out into bands, resulting in a DOS for which there is no standard formulation.

An initial analysis of the data is carried out with the DOS represented simply by a number of δ functions, whose position and amplitude are adjusted to fit the data after Gaussian phonon broadening. This approach is motivated by the observation that details in the DOS, small on a scale compared with the phonon width, are almost completely obscured by the phonon broadening. The δ functions can, thus, be thought of as representing regions with high density of states. Weak structures close to the strong peaks are summed into a single δ function, and peaks separated by a small fraction of the phonon width may well be approximated by a single δ function at the weighted average position. A small number (3–4) of δ functions generally suffices to reproduce the essential features of the data.

Note that this model is identical to one in which the δ functions are replaced by Gaussians of some arbitrary but identical width and a correspondingly reduced phonon broadening. This alternative points out a shortcoming of the δ -function model, namely, that an optimum representation of the DOS by Gaussians would contain Gaussians of different widths. Balanced against this shortcoming are the facts that the δ -function analysis keeps the number of free parameters to a minimum, provides a unique representation of the data, and allows an accurate determination of the location of regions with high DOS. The Gaussian width obtained with this representation provides an upper limit to the phonon width, and the separation of the outermost δ functions provides a lower bound to the bandwidth.

In order to obtain a better estimate of the phonon broadening and the width of the valence band, we have used another simple model, which provides a better approximation to an actual DOS. The DOS is represented by a histogram with fixed origin and bin width. The content of the bins is adjusted for an optimum fit between the phonon-broadened histogram and the experimental data. The Gaussian width, which now corresponds directly to the phonon width, remains a single additional adjustable parameter during the optimization of the structure of the histogram. Were it not for the more flexible modeling of the DOS, this representation would suffer from the same ambiguity about the phonon width as the Gaussian version of the δ -function model, because the Gaussian representation of the DOS is, in effect, replaced by the histogram. In practice, we found it necessary to exclude explicitly the Gaussian tails of the data from the histogram

(see below).

The choice of the bin width is based on experience with the δ -function model. The success of the latter is predicated on the facts that isolated peaks in the DOS remain detectable while structure with period equal to the Gaussian phonon width is almost fully attenuated. Such structure is unlikely to be recovered in the histogram-based analysis. This suggests that the bin width should be about half of the Gaussian width. That width, however, is too large to adequately specify the peak positions. Experience has shown that bin widths of the order of one-quarter of the phonon width are required. Care must then be taken to reject solutions with unphysical histogram structure, which is fully attenuated by the phonon broadening and does not manifest itself in the fit to the data. Optimization of the bin content is carried out using a conventional nonlinear least-squares algorithm and the requirement that individual bins cannot assume unphysical negative values.

The detailed structures of the histograms obtained by fitting our data are, of course, only approximations to the actual DOS because they are affected by the energy location of the bins and their width. Furthermore, the data to which the histograms are fit depend on transition probabilities across the band, which are a function of the photon energy. This latter effect is particularly noticeable in the Na salts, where valence-band data taken with different photon energies exhibit different profiles. Consistent information is obtained, however, for the energies of peaks in the DOS.

The above considerations make it clear why two different models have been used. The δ -function representation provides the most reliable approach for obtaining peak energies in the DOS, while the histogram representation is better suited for determining the DOS width.

III. RESULTS AND DISCUSSION

We have carried out our analysis using broadened δ functions and histograms for the 12 compounds shown in Table I. Using the δ -function representation, we find that three peaks suffice to fit the data for the fluoride, chlorides, and bromides, while for the iodides with larger bandwidth, four peaks are required. In the iodides, the fourth peak at smaller binding energy most likely represents the DOS near the Γ point, which is not apparent in the analysis of the other halides.

The fits obtained with this model are illustrated in Figs. 2 and 3 for NaCl and KBr, respectively. The three vertical lines are δ functions of adjustable height and position and represent the basic DOS structure. These lines are then convolved with a Gaussian of unit height and adjustable width to represent the effects of phonon broadening. The background in the NaCl data is essentially flat, except for a very weak contribution at higher binding energy associated with the 2.7-eV excitation of F centers. The background in the KBr data contains three contributions: (1) a weak, broad line at 6.5 eV binding energy due to valence-band photoemission excited by 23.1-eV radiation from the resonance lamp, (2) a very broad contribution near 10.5 eV corresponding to the

TABLE I. Binding energy of high density-of-states peaks, valence-band widths, and phonon widths in alkali halides (in eV).

	Peak binding energy (δ -function model)			Bandwidth		Phonon width	
				Expt.	Calc.	Expt.	Calc. ^a
NaF		11.66	12.09	12.86	1.60±0.20	1.5 ^b	1.10
NaCl ^c		9.66	10.30	11.18	1.80±0.18	2.1 ^b	1.16
KCl		9.19	9.52	9.98	1.20±0.15	1.1 ^b	0.76
RbCl		8.87	9.10	9.50	0.90±0.15	1.0 ^d	0.71
CsCl		8.21	8.67	9.03	1.05±0.15		0.59
NaBr	8.91	9.42	9.93	10.82	2.00±0.20	1.7 ^e	0.74
KBr		8.06	8.49	9.09	1.35±0.15	1.2 ^d	0.73
RbBr		8.19	8.55	9.09	1.20±0.15	1.0 ^d	0.68
CsBr		7.73	8.22	8.71	1.35±0.15		0.61
KI	7.55	7.88	8.34	9.19	1.80±0.18	1.7 ^f	0.68
RbI	7.41	7.64	8.05	8.87	1.65±0.15		0.66
CsI	7.03	7.43	7.79	8.54	1.65±0.15	1.8 ^g	0.61

^aCalculated from parameters in Ref. 14.

^bSee Ref. 5.

^cData taken with sample at 500 K.

^dA. B. Kunz, Phys. Status Solidi **29**, 115 (1968).

^eA. B. Kunz and N. O. Lipary, Phys. Rev. B **4**, 1374 (1971).

^fSee Ref. 16.

^gY. Onodera, J. Phys. Soc. Jpn. **25**, 469 (1968).

2.0-eV excitation energy of *F* centers, and (3) the beginning of loss structure due to excitons and interband transitions at the high-binding-energy end of the spectrum. The residuals for both NaCl and KBr fits show that the δ -function representations plus background account for every detail of the data, implying that there is no significant additional information contained in the data. The good fits obtained at the top and bottom of the band indicate that the data have Gaussian character in these

regions, i.e., the spectral shape is determined by phonon broadening, not DOS structure. This information is later used to constrain the histogram fits, so as to prevent tails in the histogram from taking over the Gaussian character of the data. Note also that this purely Gaussian character also establishes the absence of Lorentzian lifetime broadening, i.e., valence-band hole states are long lived even in the presence of nonequilibrium carriers in the conduction band during photoexcitation. The Gaussian

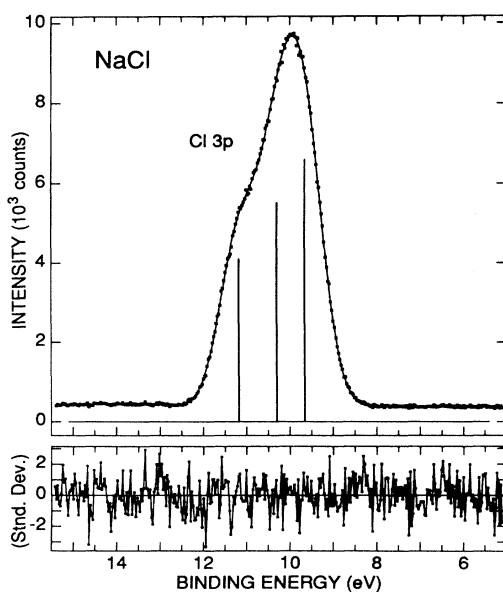


FIG. 2. Fit to valence band of NaCl, shown as a solid line through data points, using δ -function model.

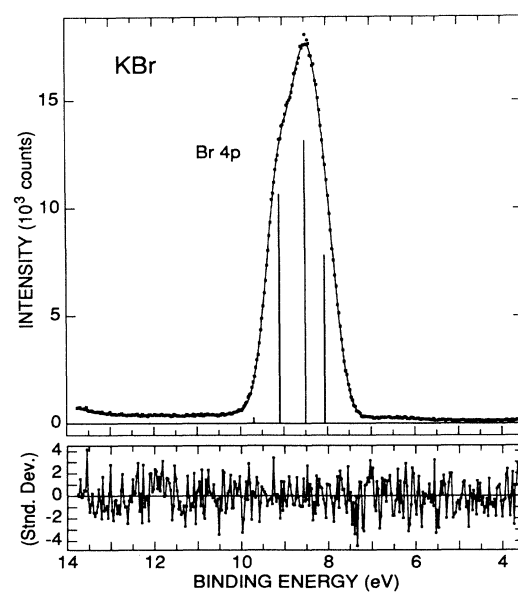


FIG. 3. Fit to valence band of KBr, shown as a solid line through data points, using δ -function model.

widths from these fits are 1.02 eV for NaCl at 500 K and 0.71 eV for KBr at 300 K.

The fact that such a skeletal, seemingly unphysical representation of the DOS yields such a good fit may seem troublesome. However, as mentioned in the previous section, this model actually represents a continuum of solutions since an arbitrary fraction of Gaussian widths (subtracted in quadrature) can be allocated to the DOS. For example, if the δ functions in KBr were replaced by Gaussians of 0.30 eV width, which would make the representation much more closely resemble a typical DOS, an identical fit would then be obtained using an additional phonon broadening of 0.64 eV. It follows that the utility of the δ -function representation is limited to locating regions with high DOS and obtaining an upper bound to the phonon broadening. The separation of the outermost peaks provides a lower bound to the bandwidth, which may be larger by a significant fraction of the phonon width. The binding energies of these high density-of-state points, given in Table I, are useful for comparison with band-structure calculations.

Since an actual DOS is not well represented by a small number of Gaussians, we turn to the histogram model of the DOS, which should give better values for the valence-band width and phonon broadening. We have used the results of the δ -function fits to define the starting point for the optimization of the histogram. This procedure has the effect of selecting solutions containing maximum phonon-width values and minimum tailing in the DOS. The resulting DOS generally bears a significant resemblance to the δ -function representations. As explained above, solutions with smaller phonon width and broader histograms, with tails that begin to take over the Gaussian character of the data, are rejected. Typical results for NaF, NaCl, and KI are shown in Figs. 4, 5, and 6, respectively.

In previous work,¹⁰ shallow *cation* core levels from these systems have been found to exhibit surface-ion shifts of ~ 0.45 eV,¹⁰ but there is no evidence here for distinguishable bulk and surface contributions in the valence band or the DOS histogram. This is really not surprising, since the shifts predicted for *anions*¹⁰ are typically only about -0.11 eV, i.e., much smaller than the phonon widths and less than the bin widths used here. The histograms, therefore, can be only very slightly broadened by this unresolved shift.

In Fig. 4, the histogram for NaF is compared to the valence-band structures taken from Ref. 5. The peaks in the DOS are in good agreement with the energies of bands at the L and X points, demonstrating that the histogram does indeed reflect the main features of the underlying DOS. The total width of the histogram is in good agreement with the dispersion from the Γ_{15} valence-band maximum to the L_1 minimum.

In Fig. 5, the histogram for NaCl is compared with the total valence-band density of states calculated by Papaconstantopoulos.¹⁵ The 2.0 eV width of the histogram is slightly smaller than the width of the calculated DOS, mainly because weak contributions at the band edges are not reproduced in the histogram. The error is comparable to the bin width. The actual measured width

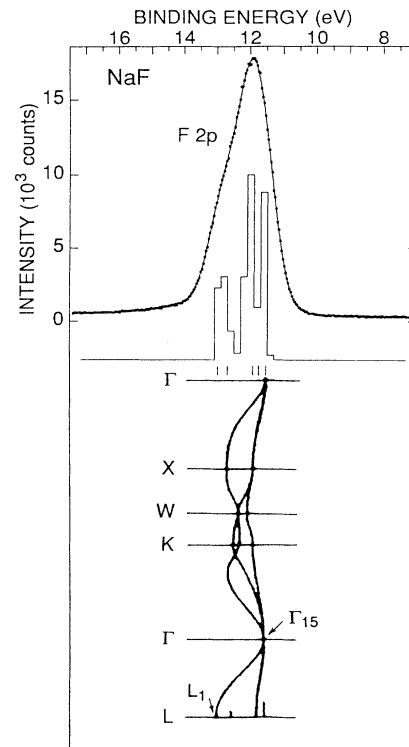


FIG. 4. Comparison between the histogram, which produces the fit to the NaF valence band, shown as a solid line through data points, and the band-structure calculation from Ref. 5.

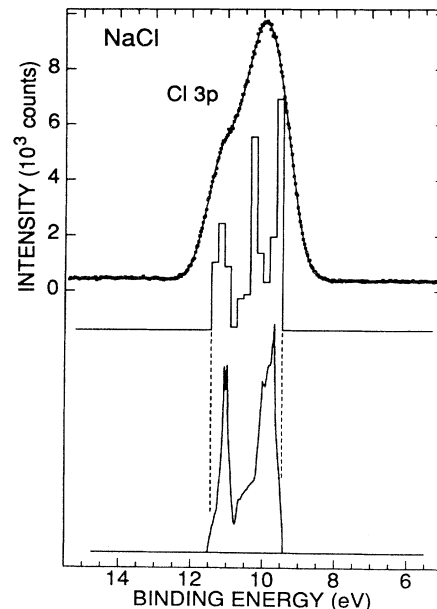


FIG. 5. Comparison between the histogram, which produces the fit to the NaCl valence band, shown as a solid line through data points, and density-of-states calculation from Ref. 15.

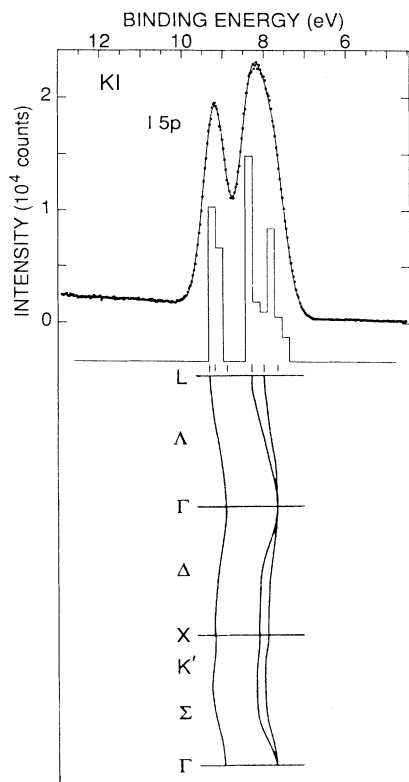


FIG. 6. Comparison between the histogram, which produces the fit to the KI valence band, shown as a solid line through data points, and the band-structure calculation from Ref. 16.

in the data is, of course, much larger still, an effect we now know to be due entirely to the 0.97-eV phonon contribution. This explains why earlier work, which overlooked this contribution and generally assumed the valence band to be equal to the full based width of the photoemission spectrum, reported excessively large values. For example, the full base width of the NaCl data is approximately 3.2 eV, while at half amplitude it is 1.95 eV. Thus, even without any analysis of the raw data, the latter value is clearly preferable because it provides, at least crudely, a way of minimizing the effect of phonon broadening.

The sharp cutoff of the calculated bands serves to clarify the rationale of using the Gaussian tails to define the phonon width, which is fundamental to the approach used in the data analysis. A comparison between the histogram and the calculated DOS shows good agreement with regard to the overall structure, but significant differences with regard to the location of some of the peaks. These differences reflect the inherent limitations of analyzing data that are so significantly phonon broadened, as explained above. It follows that the valence band and phonon widths determined by our approach are much more reliable than the detailed structure of the histograms so obtained.

A histogram representation of the KI spectrum is shown in Fig. 6. The band structure from Ref. 16 was

shifted by -0.50 eV to optimize the agreement with the experimental data. Note that the gap in the valence-band DOS is reproduced in the analysis. The largest discrepancy is at the top of the band, where the experimental histogram extends to smaller energy by the width of one bin.

The bandwidths determined from the histogram fits are summarized in Table I. We have defined this width to be the distance between midpoints of the outermost occupied bins. The uncertainty in our quoted values is then equal to the width of a single bin. Another source of uncertainty is the potential failure to detect weak parts of the DOS at the top and bottom of the band. For a given cation, the measured valence-band widths are seen to increase from chloride to bromide and iodide, clearly reflecting the change in spin-orbit splittings, which are 0.109, 0.457, and 0.942 eV for the neutral Cl, Br, and I atoms, respectively.¹⁷ The splittings in the optical spectra at the corresponding Γ points are close to these values⁶⁻⁸ and the separation of the outermost peaks obtained with the δ -function model show the corresponding increase from chloride to bromide and iodide. Comparisons between experimental and theoretical widths encounter the problem that some calculations for a given material differ by as much as a factor of 5.³ In most cases, however, the extreme values can be ignored, especially when they are at variance with results of more recent work. In Table I we show calculated bandwidths from representative band-structure calculations. The agreement is generally very good.

The experimental phonon widths shown in Table I are taken from the fits using the histogram representation. There is inevitably some ambiguity in these results, because a smaller phonon width can always be compensated by occupying additional bins at the top and bottom of the band. To avoid problems from this source, the number of occupied bins was not allowed to increase during optimization of the fit. The results are compared with theoretical phonon widths for anion core levels calculated from the parameters given by Mahan.¹⁴ Previous work¹¹ has shown excellent agreement between experimental phonon widths of cation core levels and the corresponding widths calculated from Ref. 14. In the present case, the experimental phonon width of the anion *valence states* is only $\sim 15\%$ smaller than the width calculated for *core levels*, indicating that the valence-band holes are quite localized. This finding is similar to that obtained in a study of intrinsic plasmon excitations,¹⁸ whose intensities are comparable in both core and valence photoemission data from simple metals.

IV. CONCLUSIONS

Photoemission valence-band spectra of the alkali halides are shown to be very well represented by phonon-broadened DOS histograms. These histograms,

reflecting effective DOS's because they are modified by the transition probabilities, compare favorably with band-structure calculations for the 12 alkali halides studied here. The phonon broadenings of the alkali-halide valence bands are only $\sim 15\%$ smaller than the widths calculated for anion core levels, indicating that the valence-band holes are quite localized. Surface-anion shifts, which are expected to be much smaller than the phonon width, are not resolved.

ACKNOWLEDGMENTS

We are indebted to D. A. Papaconstantopoulos for the band-structure and density-of-states calculation of NaCl shown in Fig. 5. Some of the photoemission data were obtained at the National Synchrotron Light Source, Brookhaven National Laboratory, which is supported by the Department of Energy, Division of Materials Sciences and Division of Chemical Sciences.

-
- ¹T. H. DiStefano and W. E. Spicer, *Phys. Rev. B* **7**, 1554 (1973).
²S. P. Kowalczyk, F. R. McFeely, L. Ley, R. A. Pollak, and D. A. Shirley, *Phys. Rev. B* **9**, 3573 (1974).
³R. T. Poole, J. G. Jenkins, J. Liesegang, and R. C. G. Leckey, *Phys. Rev. B* **11**, 5179 (1975); **11**, 5190 (1975) summarize the experimental and theoretical work prior to 1975.
⁴S. M. Mujibur Rahman, A. M. Harun Ar Rashid, and S. M. M. R. Chowdhury, *Phys. Rev. B* **14**, 2613 (1976).
⁵S. C. Erwin and C. C. Lin, *J. Phys. C* **21**, 4285 (1988).
⁶J. E. Eby, K. J. Teegarden, and D. B. Dutton, *Phys. Rev.* **116**, 1099 (1959); K. Teegarden and G. Baldini, *ibid.* **155**, 896 (1967).
⁷D. M. Roessler and C. W. Walker, *Phys. Rev.* **166**, 599 (1968).
⁸J. C. Phillips, *Phys. Rev.* **136**, A1705 (1964).
⁹J. M. Adams, S. Evans, and J. M. Thomas, *J. Phys. C* **6**, L382 (1973).
¹⁰G. K. Wertheim, D. N. E. Buchanan, J. E. Rowe, and P. H. Citrin, *Surf. Sci.* **319**, L41 (1994).
¹¹G. K. Wertheim, J. E. Rowe, D. N. E. Buchanan, and P. H. Citrin, *Phys. Rev. B* **51**, 13 669 (1995).
¹²P. H. Citrin, P. Eisenberger, and D. R. Hamann, *Phys. Rev. Lett.* **33**, 965 (1974).
¹³J. A. D. Matthews and M. G. Devey, *J. Phys. C* **7**, L335 (1974).
¹⁴G. D. Mahan, *Phys. Rev. B* **21**, 4791 (1980).
¹⁵D. A. Papaconstantopoulos (private communication).
¹⁶Y. Onodera, M. Okazaki, and T. Inui, *J. Phys. Soc. Jpn.* **21**, 2229 (1966).
¹⁷C. E. Moore, *Atomic Energy Levels*, Natl. Bur. Stand. Circ. No. 467 (U.S. GPO, Washington, D.C., 1952), Vols. I, II, and III.
¹⁸D. R. Penn, *Phys. Rev. Lett.* **40**, 568 (1978).